Available online at www.sciencedirect.com
SCIENCE DIRECT
ELSEVIER
Renewable Energy 30 (2005) 1101–1116
RENEWABLE ENERGY
www.elsevier.com/locate/renene

Technical note

Design and testing of a locally made loop-type thermosyphonic heat sink for stove-top thermoelectric generators

R.Y. Nuwayhid*, R. Hamade

Department of Mechanical Engineering, Faculty of Engineering and Architecture, American University of Beirut, Riad El Solh 1107-2020, Beirut, Lebanon

Received 16 July 2004; accepted 18 September 2004
Available online 23 November 2004

Abstract

The performance of a thermoelectric generator, among other aspects, depends on the use of an effective heat sink. While forced cooling using either air or water (or other coolants) is efficient, it is parasitic on the generated power and/or bulky and inconvenient. Heat pipes are known to be highly effective heat transport devices. Coupled to a thermoelectric generator, these can be used to give acceptable power output. Basing the cooling on water gives low-cost, simplicity, safety, together with good performance. In this work, the design and general performance of a small single-module thermoelectric generator configured for a stovetop waste-heat application and coupled to a locally-made thermosyphonic loop-type heat sink was undertaken. Development and performance cctesting gave mixed results and further numerical and experimental study is under way.

Keywords: Thermoelectric generator; Thermosyphonic heat sink; Stove top

1. Introduction

Thermoelectric power generation has been in existence for over 100 years. The efficiency of conversion has not managed to exceed about 10% for temperature ranges of

* Corresponding author. Fax: +961 1 744 462.
E-mail address: rida@aub.edu.lb (R.Y. Nuwayhid).

0960-1481/$ - see front matter © 2004 Elsevier Ltd. All rights reserved.
doi:10.1016/j.renene.2004.09.008

Nomenclature

C_f	friction coefficient
C_p	liquid specific heat
Dx	grid size [m]
g	gravitational acceleration [ms^{-2}]
h	heat transfer coefficient [$Wm^{-2}\,K^{-1}$]
h_{fg}	latent heat of vaporization [$kJ\,kg^{-1}$]
H_p	depth of the liquid pool [m]
K_l	liquid thermal conductivity [$Wm^{-1}\,K^{-1}$]
L	length of the thermosyphon [m]
m_c	mass flow rate of condenser cooling water [kgs^{-1}]
P	pressure [Pa]
q''	wall heat flux [Wm^{-2}]
R	inner radius of the thermosyphon [m]
r	vapor core radius [m]
Re	Reynolds number, $4\Gamma/\mu$
T	temperature [K]
u	velocity [ms^{-1}]
V	vapor condensation velocity [ms^{-1}]
x	axial distance from the top end of thermosyphon [m]

Greek symbols

δ	liquid film thickness [m]
μ	dynamic viscosity [$Ns\,m^{-2}$]
ρ	density [$kg\,m^{-3}$]
ϕ	phase change correction factor

Subscripts

a	adiabatic region
atm	atmospheric conditions
c	condenser region
e	evaporator region
l	liquid phase
p	liquid pool surface
S	saturation
w	tube wall
v	vapor phase

practical interest. Thus, power generation applications have been limited to special deep space probes (Pioneer, etc…) which use radioisotope heat sources and generate relatively low power sufficient for the task at hand. The other application is in remote power for Polar Regions, petroleum platforms or other similar instances. These systems use fossil fuel heat sources, and considering weather and other factors, may have a marginal advantage over power generating using other methods such as photovoltaics.

On the other hand, Rowe [1] has argued that when the energy input is of the waste heat type, there is a case for the use of thermoelectric conversion. In such a case, power rather than efficiency is the primary criterion. One situation where a waste heat application exists is rural domestic winter heating stoves (diesel, wood or similar). The generation of thermoelectric power from such stoves has been studied under such situations. Kilander et al. [2] considered the case of the Nordic countryside in Northern Sweden where no electric grid exists; while Nuwayhid et al. [3] assessed the case of rural Lebanon where the electric supply is generally unreliable and rural stoves are in common used in winter.

In the case of domestic stoves, the hot side temperature of a thermoelectric generator (TEG) may be considered constant on average (fluctuation especially when considering wood-fed stoves may be significant). In the coming section, it will be shown that power is proportional to the square of the temperature difference across the thermoelectric module. Thus, the task becomes to minimize the cold side temperature. Typically, the stovetop temperature would be around 200–230 °C (about 500 K). Considering, as a worst case, an average ambient temperature of 20–23 °C (293–296 K), it becomes clear that with such an application, a temperature difference of about 200 K is the limit. It is quite interesting to note that this application appears to match the range at which Bismuth Telluride (Bi_2Te_3) performs very well [4].

Based on the above, the task of decreasing the cold side temperature becomes a heat sink problem. Heat sinks for thermoelectric generators can be based either on natural convection to the ambient or on forced cooling. The simplest design is a simple finned heat sink, but in this stovetop situation it would not be capable of removing adequate heat. Adding a brushless fan is the first improvement that comes to mind. While this affords a compact and lightweight solution, the fan has to be powered by parasitically drawing from the generated power. At this stage, and because of water's superior heat transport properties, forced water-cooling comes to mind, but once again, parasitic pumping power is required. This leads to the consideration of natural cooling using water (the alternative is to use an air-cooled natural convection system but this would lead to a very large system). For compactness' sake, a closed-loop, water-based, natural circulation heat-pipe-type system is selected for building and testing.

In this work, after some introduction to thermoelectricity, heat sinks and heat pipes, a latent heat/two-phase flow Thermosyphon hereon called a Thermosyphonic heat pipe (THP) design is assessed. Designs that are similar in operational basis are found under the name of 'closed-loop two-phase Thermosyphons' (CLTPT) [5]. No attempt was made to fully ascertain the theoretical performance of an optimum system, only fabrication, assembly, and operational testing were attempted for an off-design in order to make an initial assessment of the concept.

2. Thermoelectric power

2.1. Thermoelectric generation

It is widely accepted that Seebeck first discovered the thermoelectric effect in 1822. If two dissimilar metals were to be joined such that one side is heated while

the other side is kept at a lower temperature, an electric flow will develop. The output produced was initially of a small magnitude and was of no value in direct electric power generation. With the discovery of semiconductors it was found that the output could be magnified significantly and renewed interest began around the middle of the 20th century.

The parameter giving the output voltage for a given combination of two unlike materials for a certain temperature difference is the 'Seebeck coefficient': $\alpha = \mathrm{d}V/\mathrm{d}T$. This is a property of a couple of materials but can also be written for a single material if reference is made to a material with a known thermoelectric power (E). The Seebeck coefficient for two materials being $\alpha_{12} = E_1 - E_2$. Seebeck coefficients of metals are in the range 0–50 μV/K, while that for semiconductor could be over 300 μV/K [6].

2.2. Simple power-efficiency relations of thermoelectricity

It can be shown that the power produced by a thermoelectric module to be approximately given by [7]

$$W = 2\frac{m}{(1+m)^2}\frac{\alpha^2}{\rho}N\frac{A}{L}\Delta T^2 \tag{1}$$

where $\Delta T = T_H - T_L$ is temperature difference between the hot-side temperature and the cold-side of the thermoelectric module, A is the area of a thermoelement in the module, L its length, α is the thermoelectric material Seebeck coefficient, ρ the electrical resistivity of the thermoelectric material, N the number of couples in the module, and m the electrical load ratio. It has been assumed that the Seebeck coefficient and the electrical resistivity are not temperature dependent. The equation clearly demonstrates an obvious optimization that occurs at $m = 1$ (matched load) for a selected set of material ($\alpha\rho$) and geometric (A, L) characteristics. In practice one would operate just above $m = 1$. This is because it is known that resistivity tends to increase with operation thereby decreasing m so that power will not be greatly affected over the life of a device. Also shown in the equation is the strong parabolic dependence of power on the across-module temperature difference. In this work, the open-circuit voltage is also assessed; this is easily given from the definition of the Seebeck effect by

$$V_{OC} = 2\alpha N\Delta T \tag{2}$$

where the parameters have been already defined. For a particular thermoelectric module the previous two equations can be simplified for use in the work.

2.3. Thermoelectric module selection

Several types of thermoelectric modules are available commercially. Some are optimized for cooling while other are for power generation. The difference between the two types comes from adjusting of the thermoelement length, its width, temperature tolerance of the soldering material, and the use of integrated ceramic electrical insulators on the hot and/or cold sides.

Table 1
Specifications and properties of HZ-20 module

Thermoelectric material	Bismuth Telluride (n/p)
Weight (g)	115
Cost (approx.) ($)	200
Number of couples	71
Maximum hot operating temperature (°C)	250
Leg height (mm)	5.08
Leg width (cm)	7.5
Module leg area-to-length ratio (m^2/m)	1.107
Effective thermal conductivity (W/m K)	2.4
Heat flow per unit temperature difference (W/K)	2.66
Internal electric resistance (Ω)	0.3

In this work it was decided to use the HZ-20 module manufactured by Hi-Z. Table 1 gives a listing of the major features of this module [8]. It should be noted that this module is not necessarily the only—or best—module to use in this application but is a well-tested and established module.

For the HZ-20 module (with the properties listed in Table 1), the following approximate theoretical relations for open circuit voltage, the current at maximum power, the voltage at maximum power, the maximum power (matched load condition) and the efficiency at maximum power and the maximum power conditions may be developed by using known material and geometrical characteristics [9]

$$V_{oc} = 0.026\Delta T,\ I_{mp} \approx 0.04\Delta T,\ V_{mp} \approx 0.013\Delta T$$
$$W_{max} \approx 5.0 \times 10^{-4}\Delta T^2,\ \eta_{mp} \approx 1.88 \times 10^{-4}\Delta T \quad (3)$$

These agree more or less with the actually reported performance of the HZ-20 module [8].

It should be noted that the temperature difference across the thermoelectric material in the module (ΔT) is always smaller than the measured temperature difference from the hot surface to the heat sink based mostly due to thermal contact resistance.

3. Heat sinks for stovetop thermoelectric generators

The TEG design considered was one where the hot-side temperature is normally fixed. Such a situation arises, for example in a stovetop TEG (see Refs. [2] or [3]) when temperature fluctuations due to finite wood feeding is neglected. In such a case, net maximum power will be obtained if the cold-side temperature of the TEG is minimized. This is to be achieved by improving the design of the heat sink.

Practical heat sinks for thermoelectric generators can be based either on natural convection to the ambient or on forced cooling. The simplest design is a finned heat sink, but in this situation the heat sink would not be capable of removing adequate heat since the TEG under investigation is to be placed on a stove-top. Moreover, the use of brushless fans

to cool an appropriate finned heat sink results in a compact and light solution, but the fan has to be powered by parasitically drawing from the generated power. Such a heat sink may be practical in situations where high power is generated using several modules. If a temperature difference of 100 °C is acceptable, a third reasonable alternative although relatively large system could be an 'open pan' heat sink [10] where the heat sink consists simply of an open-topped pan full of water. While this design draws on the large latent heat of vaporization of water, it suffers from the need for regular attention to prevent dry-out.

On the hand, and in order to obtain large temperature differences, the authors will consider heat pipes for cooling purposes. The use of refrigerant-based heat pipes is very effective. However, due to the intended domestic use of the TEG design at hand, safety precludes the use of these coolants. This is because failure of the heat pipes in heat removal could lead to very high pressures. While forced water-cooling is another alternative, once again pumping power is required. This leads to the consideration of natural cooling using water (the alternative is to use an air-cooled natural convection system but this would lead to a very large system). Heat pipes are very efficient but a little difficult to operate. A closed-loop heat pipe is a simpler and more flexible alternative. Even if not operating as a heat pipe such a design can still cool as it operates in a simple thermosyphonic mode. In fact, in the very worst situation, the loops may even cool to some degree as simple extended surfaces. In this paper a water-based thermosyphonic close loop heat pipe (THP) system, also called in general a 2-phase closed loop Thermosyphon, is designed, built and assessed as part of a thermoelectric generator for use on domestic stove tops.

4. Thermosyphonic heat pipe design

4.1. Description

In order to try to achieve higher ΔT's, designs using latent heat exchange (heat pipes) were considered. Since the required design had to be inherently safe it was decided (for the present) to avoid using refrigerants such as R-22. Instead, water was the selected working fluid for several reasons. By using water, high-pressure differences are avoided, leading to lower hoop stress and hence an increased safety-factor. Additionally, water has a high latent heat of vaporization (2333.8 kJ/kg at 70 °C which is the selected design operating temperature—much more heat could be removed by the same mass of water as compared to R-22). At this temperature, the saturation pressure is 31.19 kPa (0.31 atm). Furthermore, water is in the liquid phase at room temperature and therefore the pipe is filled with the desired amount of liquid accurately and according to the design calculations.

With water as the working fluid, the challenge was to build a device that gives a ΔT of 100 °C or more across the thermoelectric module while being safe and self-contained (closed-loop). Normal vertical heat pipe designs were considered but, thermosyphonic designs, which operate on the same principal, were opted for instead. A possible advantage of a Thermosyphonic Heat Pipe (THP) over normal heat pipes is that they operate clearly

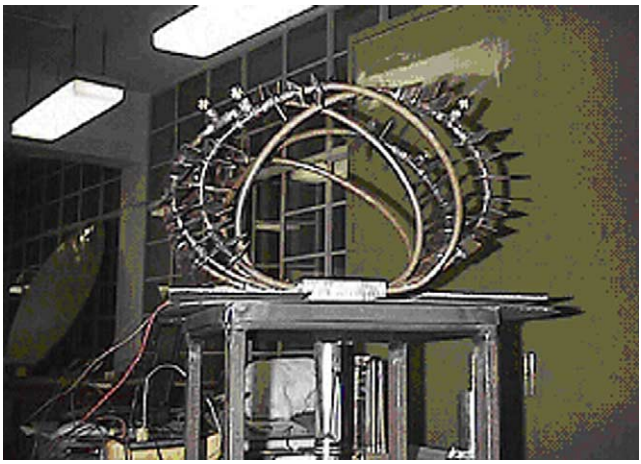

Fig. 1. Photograph of the THP/TEG on the Bunsen burner platform.

as continuous closed loop systems. Thus, in the event of failure, they still present an area large enough to provide sufficient cooling and prevent large pressure build-up. In addition, the thermal inertia of water assists in this safety feature. Water in a THP would evaporate in the evaporator side, circulate through the loop, cool on the condenser side, and condense back to the evaporator side. Hence no wick is needed to help liquid return to the evaporator. Fig. 1 shows a photograph of the TEG with the THP loops clearly visible while Fig. 2(a) and (b) show two schematics of the TEG.

4.2. Theoretical model of a THP

4.2.1. Theoretical background

In order to place bounds on the design and in order to arrive at a preliminary sizing, a theoretical model for the thermal performance of a two-phase heat sink attached to a thermoelectric module was first set-up. The heat sink was assumed to behave like a straight annular two-phase thermosyphonic heat pipe. Zuo and Gunnerson [11] modeled such a system. Their model assumes one-dimensional, steady state Newtonian flows for both phases. A more pertinent model that will be applied in a coming work would be that of Haider et al. [5] where a closed-loop two-phase thermosyphonic model was studied and describes a setup quite similar to the present TEG heat sink with the presumed assumption in [5] that two-phase flow will always exist. Nevertheless, for the current evaluation, the authors use a (simpler) straight heat pipe model and which gives some guidelines for the design of the prototype TEG heat sink.

The model of Zuo-Gennerson [11] was implemented in Matlab. It and solved for different evaporator-to-condenser ratios (L_e/L_c) ratios considering a constant saturation temperature (taken to be 343 K in this experiment). The evaporator was assumed to be heated at a constant heat flux. Fig. 3 shows the existence of an optimum value for L_e/L_c that corresponds to a maximum heat removal using the Thermosyphon.

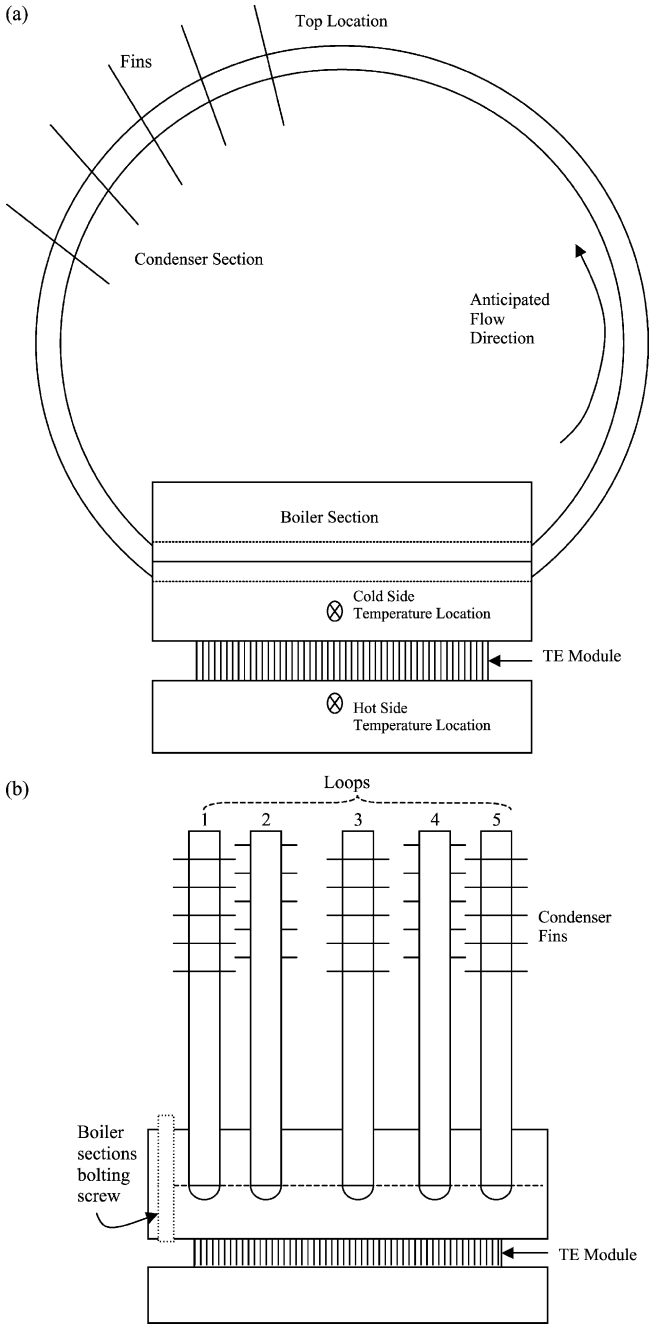

Fig. 2. (a) Schematic of THP/TEG showing one of the thermosyphonic loops. (b) Schematic of the THP/TEG showing a side view of the 5 loops.

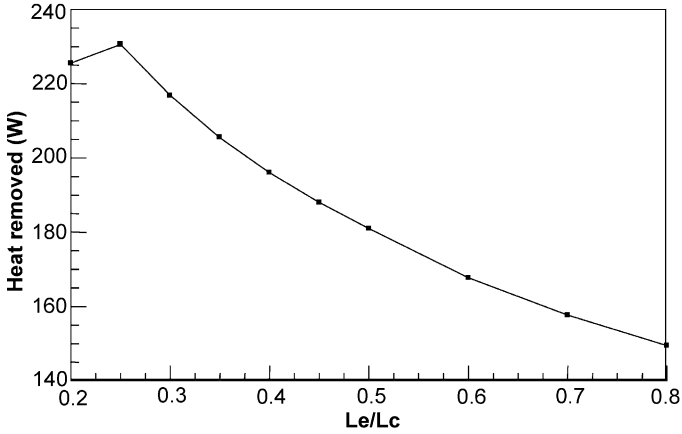

Fig. 3. Heat removed by the THP versus ratio of evaporator to condenser length.

In this application, the thermosyphon is used to cool a thermoelectric device (module plus edge of hot side) of width 10 cm. Thus, for an evaporator length of $L_e = 10$ cm, the corresponding optimum condenser length is $L_c = 40$ cm from Fig. 3. This figure results in a bulky design and a decision to set $L_e/L_c = 0.5$ was therefore taken leading to a condenser length of $L_c = 20$ cm.

The TEG cold plate (which is the evaporator section of the THP) is conservatively designed with a heat flux of 700 W (see Hi-Z specifications table at $\Delta T = 150$ K). Considering the dimensions of the TEG (above), the number of THP loops that can be installed is limited to 5. Thus, each THP loop must theoretically remove 140 W. From Fig. 3, for $L_e/L_c = 0.5$, the heat removed per loop is about 185 W which is slightly higher than required. Appendix shows a simple evaluation of the heat removal capability of the condenser section of THP and the finning requirement in order to assure natural circulation. Furthermore, this calculation justifies the selection of water since the heat input is greater than the nucleation heat of water.

4.3. Manufacturing the THP

A 75 cm length of a 3/8-inch (9.5 mm) soft copper pipe was bent into a shape such that the evaporator section would be directly over the heating plate (the TEG cold plate), whereas the finned condenser section would be kept staggered out of the heated column. This configuration insured that the condenser always be cooler than the evaporator is and that the vapor does not circulate in an undesirable direction.

Since a 12×10 cm plate with five loops had to be cooled, the holes drilled in the plate were so close that there would not be enough space to install the fins. To solve this problem, the authors decided to install the loops in an alternating manner—i.e. the evaporator side of one loop is surrounded by the condensers of the adjacent loops. This disposition of the loops also guaranteed a static equilibrium of the device since the total mass of the fins was considerable.

The loops were to be clamped between 2 aluminum plates drilled especially for that purpose. To minimize thermal contact resistance, thermal grease was used. The main advantages of this plate/loop design were (1) simplicity in attachment/replacement of a loop and (2) reduction of necessary welding operations (thus minimizing the possibility of leakage). The selection of the aluminum for the plates was based on the easy machining of aluminum compared to copper (although at a lower thermal conductivity) in addition to reduced weight.

Manufacturing was unexpectedly easy. The loops were to have no sharp edges to avoid high-pressure gradient and tube distortion. A wooden mold was utilized to give the loops their final shapes. The fins (10 required per loop) were made of copper sheets drilled and welded in to the pipes. The small spacing between the fins made the welding process difficult to achieve. Once the fins installed, T-fittings were to join the ends of the pipe.

A valve was welded on the third opening of the *T*. The same operation was performed on the five loops. The hole diameter in the aluminum plates (the loop base) was drilled deliberately slightly smaller than the pipes diameter. This, in addition to thermal grease, reduces the thermal contact resistance between the aluminum plates and the copper tubes.

On the 'hot' aluminum plate, thermal grease was spread and a thin alumina ceramic electric insulating sheet was placed. Again, on top of this sheet thermal grease was spread. The HZ-20 module was then placed over the sheet. Thermal grease was spread on both sides of another alumina ceramic sheet, which was placed on top of the module. The cooling section (including the THP loops) base was then placed onto the rest of the assembly and four steel screws are used to secure the assembly.

4.4. Filling the THP

The high surface tension of water and the small cross section of the valve prevented normal filling of the pipes with the usual graduated cylinder. To overcome this, a syringe was used. After filling the loop pipes with 10 ml of pure water, they were evacuated, using a vacuum pump until the pressure in the loop pipes reached values of 4.5–7.3 psi (0.3–0.5 atm).

4.5. Experimental testing of THP

4.5.1. Preliminary and open circuit tests

Initially frequent repeated runs were performed in order to note performance dependencies and sensitivities and to ascertain the devices general capability. In addition, to a Bunsen burner heated platform, runs were also done using an electric hotplate as well as a specially designed rig using electric heating elements. Table 2 shows 7 runs and indicates the mixed results that were obtained under different thermosyphonic loading conditions. The results in the table show the cooling loops to be operating in different regimes of operation ranging from possible thermosyphonic latent heat transfer to simple fins. Achieved cold side temperatures were never less than 108 °C while achieved open circuit voltages ranged from 1.57 to 1.90 V indicating very similar temperature differences although at different loop operating conditions. Fig. 4(a) and (b) show the hot side, cold

Table 2
Repeated runs with different loadings and different heating platforms

Run	ΔT_{HC}	V_{OC}	ΔT_{TE}	$T_{tube,top}$	Water loading	$T_{ambient}$	Heater
1	109.8	1.80	69.2	60	10 ml	23.5	Hotplate
2	105.0	1.85	71.1	76	Empty	24.0	Hotplate
3	137	1.90	73.0	99	8.5 ml	21.5	Hotplate
4	106	1.72	66.1	45	16.0 ml	21.0	Hotplate
5	99	1.61	61.9	79	16.0 ml	22.2	Bunsen burner
6	95	1.57	60.3	88	15.0	23.5	Bunsen burner
7	111	1.9	73.0	35	15.0	21.5	Heating elements

side, condenser outlet, loop-top and boiler outlet temperatures for the case of empty (unfilled-open) loops and for loops with 10 ml of water. With 10 ml. filled loops the hot side and cold-side temperatures are shifted higher than for the empty case although the temperature difference is very similar. It would appear that the water is retarding the heat removal and causing higher temperatures in general. This is clearly reflected in a lower loop-top temperature with the 10 ml fill. It may be that the water stores heat that would be transported otherwise by conduction to the loop tops. This shows that the loop heat sinks may not always work as a true two-phase system. Nevertheless, it is being assessed.

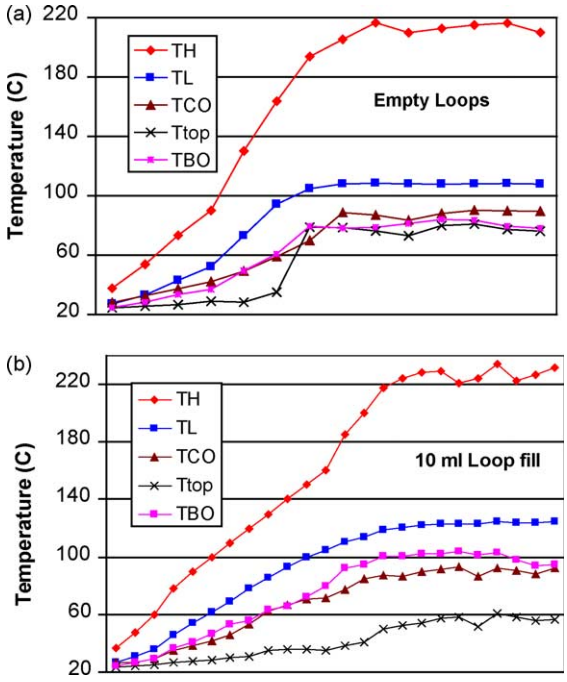

Fig. 4. (a) Temperature versus arbitrary time for a run with empty loops. (b) Temperature versus arbitrary time for a run with 10 ml water fill per loop.

Having assessed general tendencies, a further run using the Bunsen burner platform was undertaken using 10 ml water loading per loop. This leads to a measured temperature difference of 93 °C between the hot plate and the cold plate. However, upon scrutiny of the evolution of the temperatures of tubes 3 and 4 (the five loops are numbered one through five consecutively), it was concluded they were operating as simple fins. A probable reason for this was a leak in the pipes bringing back the pressure to atmospheric pressure. This being the case, evaporation would not take place before the tube temperature reaches 100 °C. A pressure gage read atmospheric pressure and confirmed the previous assumption. The faulty valves were then replaced and the loops in question were evacuated once again. A second testing was performed with the five loops were verified to be working as expected. A measured temperature difference (different from the true difference) between hot plate and cold plate of 130 °C was achieved.

Before proceeding to the optimum power test, the THP design was run in the open-circuit mode for over an hour. The open circuit voltage was measured as 2.55 V. Using Eq. (2), the true temperature difference across the HZ-20 module is found to be $\Delta T_{\text{avg, one hour}} = 94$ °C. Since the measured temperature difference was about 130 °C, a thermal contact loss of about 36 K is apparent. This difference may be assumed to be equally apportioned between the hot and cold side contacts of the module.

The behavior of the THP was then studied in more detail. It was noted that before the evaporator of a loop reaches a temperature of about 70 °C, it would be behaving as a simple fin. When the evaporator's temperature reaches 70 °C, the loop is expected to start working as a thermosyphon with latent heat transfer. The evaporator's temperature always stays somewhat higher than that of the condenser and this verifies that the vapor circulation is in the correct direction form evaporator to condenser. To be sure that the loop is behaving as a thermosyphon the top temperature must be close to the boiler and condenser temperatures and not lag far behind them. If the top temperature for a loop remains low (i.e. 40–50 °C), then that loop is not behaving as a thermosyphon but as a simple fin.

The temperature variation of the 5 loops along the evaporator, the condenser and the top were monitored. Fig. 5(a) and (b) shows the performance of loop 2 and loop 3 (see figure for loop labeling). The temperatures evolution of Loop 2 appears to indicate normal thermosyphonic functioning. Loop 3 was the last tube to start working as a thermosyphon. Until 53 m in the run, loop 3 showed a behavior more typical of a simple fin with a relatively low top temperature compared to loop 2 which by that time was behaving as a thermosyphon with a top temperature very close the 70 °C. At 53 m the top temperature loop 3 rose from about 45 °C to almost 68 °C verifying that loop 3 initiation of thermosyphonic operating conditions.

4.5.2. Power test

In order to fully test the steady perfornmance of the TEG/THP, a 2-h test run was performed. Using the bunsen-burner heating platform, an initial heat-up period of 45 m was allowed. At that stage a V_{OC} of 1.9 V was measured. The indicated T_H and T_L were measured as 195 and 100 °C, respectively. Making use of Eq. (2), the true ΔT is 70 K (rather than 95 K), so that $T_{H,true} = 182.5$ and $T_{L,true} = 112.5$ °C.

The temperatures of the top of each of the 5 THP loops were taken and found to be for loops 1–5 as follows: 88, 83, 82, 80 and 79 °C, respectively. While difficult to ascertain

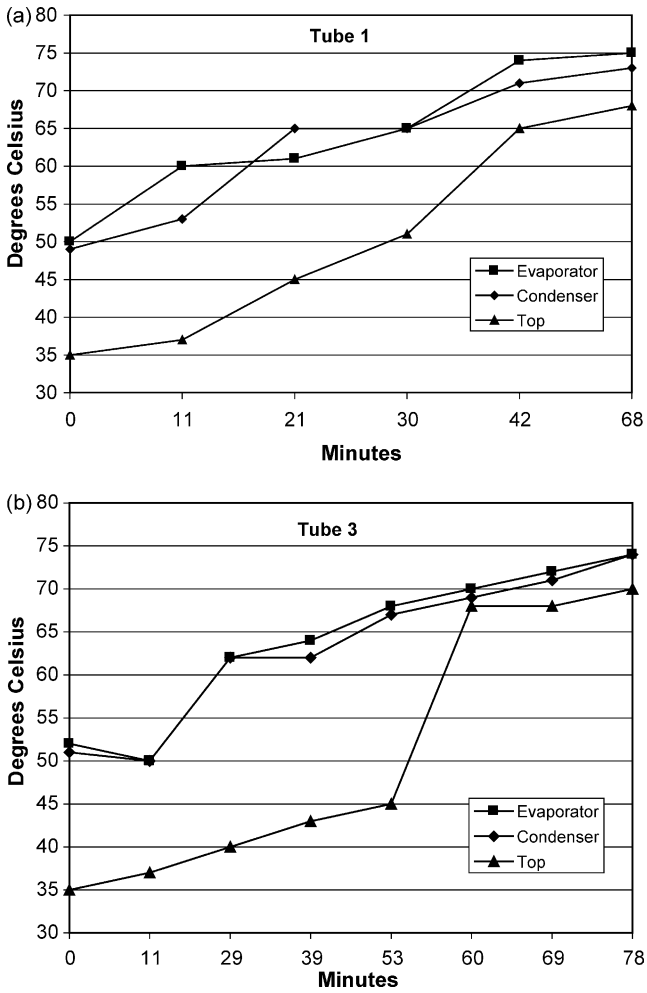

Fig. 5. (a) Thermal performance of loop 2 during a full thermoelectric run. (b) Thermal performance of loop 3 during a full thermoelectric run.

the performance of the loops properly, a check on the boiler side versus the condenser side of the TEG cold plate showed a temperature difference of several degrees. This appears to indicate that the THP loops are indeed operating and not merely functioning as fins.

After 1.5 h from startup a load test was performed. The indicated hot and cold temperatures were stable at 212 and 102 °C, respectively. Fig. 6 shows the voltage-current performance from an open circuit voltage of 2.09 V to the short-circuit current condition. The maximum power condition was found to be $V_{mp} = 0.96$ V and $I_{mp} = 2.96$ A, so that the maximum power is 2.84 W. From V_{OC}, the true ΔT is 77 K and the true T_H and T_L are 196 and 118 °C. A comparison with the theoretical predictions of Eq. (2) shows satisfactory agreement.

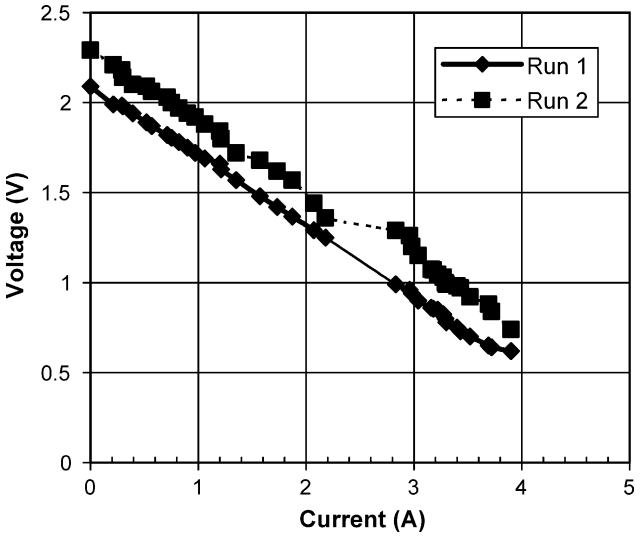

Fig. 6. Voltage-current performance load test runs for THP/TEG.

A second load test was performed when the indicated hot and cold temperatures were 236 and 109 °C, respectively ($\Delta T_{\text{indicated}} = 127$ K). The open-circuit voltage was 2.29 V, so that the true temperature difference, hot temperature and cold temperatures were 85, 215, and 130 °C, respectively. Fig. 6 also shows this second test that serves as an upper temperature capability run. For this second run V_{mp}, I_{mp} and maximum power are 1.07 V, 3.18 A and 3.40 W, respectively. For this run, a check on the THP loops top temperatures was done and showed consistency in the range 90–93 °C. The increase over the values of the previous run is expected since the current run has higher temperatures than the heat removal system was designed for.

5. Conclusions

A heat sink composed of thermosyphonic heat pipe for a stovetop thermoelectric generator has been proposed, built, and tested. The design was simple, of low cost, and well matched to a rural stove application. Using a commercially available module and no fan-assisted cooling, tests gave over 3 W of power at about 1.0 V and 3 A with a temperature difference of 70–80 K. The rather low ΔT achieved indicated some problems related to filling and sealing of the THP thermosyphonic loops. Further work on the THP design could result in true latent heat removal and hence higher ΔT's.

Acknowledgements

The authors would like to thank Mrs B. Asmar, R. Nassar, and M. Zreik for their active role in converting the THP design into a working device. Dr A. Shihadeh for his valuable suggestions and observations.

Appendix

In order for the thermosyphon to be self-sufficient for a relatively long period, an adequate fin model was needed where the rate of water condensation equals to the rate of evaporation. For the thermosyphon to operate, an amount of heat higher than the heat of nucleation of the water is required. The nucleate boiling heat flux is given by [12].

$$\dot{q}_{\text{nucleate}} = \mu_{\text{l}} h_{\text{fg}} \left[\frac{g(\rho_{\text{l}} - \rho_{\text{v}})}{\sigma}\right]^{1/2} \left[\frac{C_{\text{pl}}(T_{\text{s}} - T_{\text{sat}})}{C_{\text{sf}} h_{\text{fg}} \text{Pr}_{\text{l}}^{n}}\right]^{3}$$

where μ_{l} is the viscosity of the liquid, h_{fg} is the enthalpy of vaporization, ρ_{l}, ρ_{v} is the densities of the liquid and the vapor, σ is the surface tension of liquid–vapor interface, C_{pl} is the specific heat of the liquid, T_{s} is the surface temperature of the heater, T_{sat} is the saturation temperature of the liquid, C_{sf} is the experimental constant that depend on surface-fluid combination, Pr is the Prandtl number of the liquid, n is the experimental constant that depends on the fluid. In the current case, the values in the equation are

$$\mu_{\text{l}} = 0.404 \times 10^{-3} \text{ kg/(m s)},\ h_{\text{fg}} = 2333.8 \times 10^{3} \text{ J/kg},\ g = 9.81 \text{ m/s}^2$$

$$\rho_{\text{l}} = 977.5 \text{ kg/m}^3,\ \rho_{\text{v}} = 0.1988 \text{ kg/m}^3,\ \sigma = 0.06445 \text{ N/m}$$

$$C_{\text{pl}} = 4190 \text{ J/(kg }^{\circ}\text{C)},\ T_{\text{s}} = 79\ ^{\circ}\text{C},\ T_{\text{sat}} = 70\ ^{\circ}\text{C},\ C_{\text{sp}} = 0.0130$$

$$\text{Pr} = 2.55,\ n = 1.0, q_{\text{.nucleate}} = 41964 \text{ W/m}^2$$

This works out to about 100 W heat input per loop.

The flow regime in natural convection is governed by the Grashof number $\text{Gr} = (g\beta(T_{\text{s}} - T_{\infty})\delta^3/v^2)$, where g is the gravitational acceleration, β is the coefficient of volume expansion, (equals $1/T$ for ideal gases), δ is the characteristic length of the geometry, v is the kinematic viscosity of the fluid. Now assuming natural convection over the fin as if over a horizontal surface, then $\text{Nu} = 0.59\ \text{Ra}^{1/4}$ and $\text{Ra} = \text{Gr} \times \text{Pr}$.

In the current case, $T_{\text{film}} = \frac{T_{\text{fin}} + T_{\infty}}{2} = \frac{70+30}{2} = 50^{\circ} = 323$ K and $\text{Ra} = 2.68 \times 10^9 \times L_{\text{ch}}^3$.

Hence, $\text{Nu} = 0.59\text{Ra}^{1/4} = 134.2 L_{\text{ch}}^{3/4}$ But, $h = \frac{K}{L_{\text{ch}}}\text{Nu} \Rightarrow h = \frac{3.7}{L_{\text{ch}}^{1/4}} \Rightarrow L_{\text{ch}} = \frac{V}{A} = 5 \times 10^{-4}$.

For $w_{\text{fin}} = 10$ cm, $t = 1$ mm (set by our design).

Hence $h = 24.6$ W/m^2 °C.

Assuming a fin efficiency of 90%, $\zeta = 0.15$ (Ref. [2], Fig. 3.69).

$$\zeta = (L + 1/2\ t)\sqrt{h/Kt} \quad L = 0.019 \text{ m} \sim 2 \text{ cm}$$

$$\dot{Q}_{\text{total}} = \dot{Q}_{\text{nucleation}} + \dot{Q}_{\text{vaporization}} \Rightarrow \dot{Q}_{\text{vaporization}} = 140 - 100 = 40 \text{ W}$$

$$\dot{Q}_{\text{vaporization}} = \dot{Q}_{\text{condensation}} = \dot{Q}_{\text{unfinned}} + \dot{Q}_{\text{finned}}$$

$$\dot{Q}_{\text{vaporization}} = (h\pi s \Delta T)(n-1) + 2nhA_{\text{fin}}\Delta T$$

where n = number of fins, and s = spacing between fins.

After iterating between n and s,
For $n=10$, $s_{\min}=1.4$ cm. For the sake of the welding process, we took $s=2$ cm.
So the fin dimension is 10 cm by 2 cm.

References

[1] Rowe DM. Recent developments in the thermoelectric recovery of low temperature waste heat, Fourth International Conference On New Energy Systems and Conversions, Osaka University, June 27–30, 1999; p. 307–15.
[2] Killander A, Bass J. A stove-top generator for cold areas, Proceedings of 15th International Conference on Thermoelectrics, Pasadena, CA, USA, 1996; p. 390–3.
[3] Nuwayhid RY, Rowe DM, Min G. Low cost stove-top thermoelectric generator for regions with unreliable electricity supply. Intl J Energy Res 2001 (In review).
[4] Rowe DM. Thermoelectric Power Generation—An Update, 9th Cimtec—World Forum on New Materials, Symposium VII. In: P. Vincenzine editor, Innovative Materials in Advanced Energy Technologies, 1999.
[5] Haidar SI, Joshi YK, Nakayama W. A natural circulation model of the closed-loop, two-phase thermosyphon for electronics cooling. J Heat Transfer 2002;124.
[6] Rowe DM. Thermoelectric Power Generation—An Update, 9th Cimtec—World Forum on New Materials, Symposium VII—Innovative Materials in Advanced Energy Technologies, p. 649–664, Florence, Italy, 1998.
[7] Min G, Rowe DM. Peltier devices as generators. CRC Handbook of Thermoelectrics. London: CRC Press; 1995. Chapter 38.
[8] HZ-20 Thermoelectric Module description, Hi-Z Online brochure, www.hiz.com, Hi-Z Technology Inc., San Diego, CA.
[9] Nuwayhid RY, Shihadeh A, Ghaddar N. Development and testing of a domestic woodstove thermoelectric generator with natural convection cooling. Energy Conversion Manage 2004 (In review).
[10] Nuwayhid RY, Moukalled F, Abu said R, Daaboul M, Rowe DM, Min G. Practical design considerations for a rural stove-top thermoelectric generator, 19th Internal Conference on Thermoelectricity (ICT 2000) August 20–24, 2000.
[11] Zuo ZJ, Gunnerson FS. Numerical modeling of the steady-state two phase closed Thermosyphon. Int J Heat Mass Transfer 1994;37(17):2714–22.
[12] Incropera FP, DeWitt DP. Fundamentals of heat and mass transfer, 4th ed. London: Wiley; 1996 p. 543–5.